



## The microbial network property as a bio-indicator of antibiotic transmission in the environment

Qun Gao<sup>a</sup>, Shuhong Gao<sup>b</sup>, Colin Bates<sup>c</sup>, Yufei Zeng<sup>a</sup>, Jiesi Lei<sup>a</sup>, Hang Su<sup>a</sup>, Qiang Dong<sup>d</sup>, Ziyang Qin<sup>a</sup>, Jianshu Zhao<sup>e</sup>, Qiuting Zhang<sup>c</sup>, Daliang Ning<sup>c</sup>, Yi Huang<sup>f</sup>, Jizhong Zhou<sup>a,c,g</sup>, Yunfeng Yang<sup>a,\*</sup>

<sup>a</sup> State Key Joint Laboratory of Environment Simulation and Pollution Control, School of Environment, Tsinghua University, Beijing 100084, China

<sup>b</sup> School of Civil and Environmental Engineering, Harbin Institute of Technology (Shenzhen), Shenzhen 518055, China

<sup>c</sup> Institute for Environmental Genomics and Department of Botany and Microbiology, University of Oklahoma, Norman, OK 73019, USA

<sup>d</sup> Institute of Chemical Defense, Beijing 102205, China

<sup>e</sup> School of Biological Sciences, Georgia Institute of Technology, Atlanta, GA 30318, USA

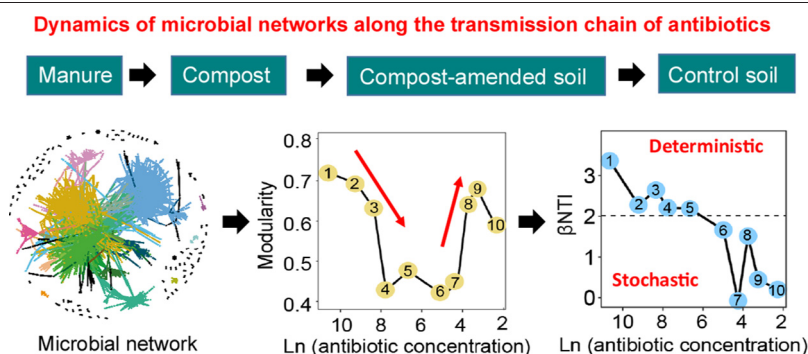
<sup>f</sup> State Key Joint Laboratory of Environmental Simulation and Pollution Control, College of Environmental Science and Engineering, Peking University, Beijing 100871, China

<sup>g</sup> Earth Sciences Division, Lawrence Berkeley National Laboratory, Berkeley, CA 94720, USA

### HIGHLIGHTS

- Bacterial taxonomic compositions changed from the dominance of *Firmicutes* to *Proteobacteria* alongside antibiotic transmission.
- Ofloxacin and tetracycline were most predictive antibiotics for bacterial and functional network properties, respectively.
- Modularity was consistently much higher in functional networks than bacterial networks.
- Modularity of association networks can be an indicator of system stability for microbial communities.
- Microbial community assembly is one of the primary mechanisms underlying microbial interactions.

### GRAPHICAL ABSTRACT



### ARTICLE INFO

#### Article history:

Received 22 July 2020

Received in revised form 18 October 2020

Accepted 10 November 2020

Available online 14 November 2020

Editor: Fang Wang

#### Keywords:

Antibiotics

Bacterial networks

Functional networks

Modularity

Community assembly

### ABSTRACT

Interspecies interaction is an essential mechanism for bacterial communities to develop antibiotic resistance via horizontal gene transfer. Nonetheless, how bacterial interactions vary along the environmental transmission of antibiotics and the underpinnings remain unclear. To address it, we explore potential microbial associations by analyzing bacterial networks generated from 16S rRNA gene sequences and functional networks containing a large number of antibiotic-resistance genes (ARGs). Antibiotic concentration decreased by more than 4000-fold along the environmental transmission chain from manure samples of swine farms to aerobic compost, compost-amended agricultural soils, and neighboring agricultural soils. Both bacterial and functional networks became larger in nodes and links with decreasing antibiotic concentrations, likely resulting from lower antibiotics stress. Nonetheless, bacterial networks became less clustered with decreasing antibiotic concentrations, while functional networks became more clustered. Modularity, a key topological property that enhances system resilience to antibiotic stress, remained high for functional networks, but the modularity values of bacterial networks were the lowest when antibiotic concentrations were intermediate. To explain it, we identified a clear shift from deterministic processes, particularly variable selection, to stochastic processes at intermediate antibiotic

\* Corresponding author.

E-mail address: [yangyf@tsinghua.edu.cn](mailto:yangyf@tsinghua.edu.cn) (Y. Yang).

concentrations as the dominant mechanism in shaping bacterial communities. Collectively, our results revealed microbial network dynamics and suggest that the modularity value of association networks could serve as an important indicator of antibiotic concentrations in the environment.

© 2020 Elsevier B.V. All rights reserved.

## 1. Introduction

The excessive use of antibiotics, which is widely occurring, promotes the proliferation of antibiotic resistance genes (ARGs). Environmental dissemination routes for ARGs have been widely reported to be important for the spread of antibiotic resistance (Bengtsson-Palme et al., 2017; Bengtsson-Palme and Larsson, 2015). ARGs can evolve, mobilize, transfer and disseminate in diverse environmental settings, such as livestock gut and manure (Allen, 2014; Bengtsson-Palme, 2017), sewage treatment plants (Bengtsson-Palme et al., 2016; Rizzo et al., 2013), water bodies (Bengtsson-Palme et al., 2014; Cabello, 2006), biofilm (Lundström et al., 2016) and the food supply chain (Bengtsson-Palme et al., 2017; Rolain, 2013). Considering that ARGs could spread among bacterial taxa by horizontal gene transfer, intimate interactions among taxa could lead to substantial antibiotic resistance, which poses a public health risk for challenges in treating pathogenic infections. For example, contamination of river waters by quinolones has promoted the transfer of chromosomally encoded *qnr* genes to the plasmid, resulting in resistance of new bacterial hosts to quinolones (Poirel et al., 2005). Bacteriophage-host interactions act as vectors for the horizontal gene transfer of ARGs among bacteria, whereby the phage carries a genetic trait from a donor bacterial cell to a recipient cell (Balcazar, 2014). Therefore, understanding how interaction among bacterial taxa enables the spread of antibiotic resistance and gives rise to dynamic population behaviors is a fundamental issue in environmental science (Kelsic et al., 2015). Nonetheless, the mechanisms of microbial interactions that contribute to antibiotic resistance remain elusive in complex environments.

The application of manure to agricultural soils remarkably increases antibiotic residues, ARG abundance, and antibiotic-resistant bacteria (ARB) population in soils (Zhang et al., 2020). Fifteen-year application of manure to soils largely increased the abundance of indigenous soil ARGs and mobile genetic elements that further facilitate the spread of ARGs (Wang et al., 2020). Although composting could effectively reduce ARG abundance (Zhang et al., 2020), the residues of antibiotics in compost products may still pose selection pressure for the evolution of ARGs and ARB (Y.-J. Zhang et al., 2019). The ARG abundance in root endophyte and rhizosphere was increased after manure and compost application (Zhang et al., 2018), revealing ARG transmission from manure to agricultural soils. Those studies provide a strong rationale for the transmission of ARGs and ARB from manure/compost to agricultural soil and other soil environments.

A closely related question is how microbial interactions evolve along the environmental transmission of antibiotics. At high antibiotic concentrations, antibiotics support the survival of microorganisms by serving as 'defense weapons' against competitors (Linares et al., 2006; Macheleidt et al., 2016), which benefits individuals but comes at the expense of reducing population diversity and stability (Xavier, 2011). At low antibiotic concentrations, antibiotics serve as signaling molecules that regulate homeostasis of microbial communities by stimulating inter-species and intra-species communication or by conferring an advantage in nutrient acquisition (Goh et al., 2002). Consequently, microbial interactions may be enhanced. Low concentrations of antibiotics can also induce biofilm formation, increase bacterial motility, and trigger secreting virulence factors required for pathogenesis (Linares et al., 2006; Rumbaugh et al., 2009). Considering that the antibiotic transmission chain varies by antibiotic concentrations, investigating microbial dynamics along the transmission chain provides an important opportunity for evaluating the different roles of low and high antibiotic concentrations in antibiotic resistance development.

Association networks have recently been used to identify keystone ARGs, functional groups, and biochemical pathways that act in concert to modulate bacterial responses to antibiotics (Gardner et al., 2003; Kohanski et al., 2007; Kohanski et al., 2008). In a simulated network, antibiotic-degrading taxa attenuated the inhibitory interactions between antibiotic-producing taxa and antibiotic-sensitive taxa (Kelsic et al., 2015). Such three-way interactions among taxa were also observed in biofilms in a laboratory experiment (Narisawa et al., 2008). In another network study, *tetM* and aminoglycoside resistance genes were identified as keystone genes that can be used to quantitatively estimate the abundance of 23 other co-occurring genes responsible for aminoglycoside, bacitracin, and  $\beta$ -lactam resistance (Li et al., 2015). These findings provide novel insights into potential interactions among ARGs and their possible hosts beyond common analyses of community diversity and composition.

Methods of ecological process analyses have been developed to explain the phylogenetic assembly of microbial communities (Stegen et al., 2013; Zhao et al., 2019). Both deterministic (e.g., abiotic or biotic selection) and stochastic processes (e.g., birth, death, and immigration) are essential in shaping microbial interactions (Z. Zhang et al., 2019; Zhou et al., 2014). For example, high antibiotic concentrations in the environment could impose severe stress on the microbial community so that cooperation among microorganisms is necessary for survival (Hui et al., 2013). In comparison, microbial interactions in a less stressful environment could change with random birth-death events, colonization, and immigration (Ning et al., 2019). However, it has seldom been examined whether deterministic or stochastic processes play dominant roles in affecting microbial interaction along the environmental transmission chain of antibiotics.

In this study, we collected manure samples in five swine farms located in the suburban area of Beijing, China. As animal manure is regularly treated by aerobic compost before applying to agricultural fields, we also took compost samples and compost-amended agricultural soils. Since compost-amended agricultural fields can potentially affect neighboring soils, we collected agricultural soils without compost amendment from the same agricultural field. Along this environmental transmission chain, antibiotic concentrations decreased rapidly from 16,761  $\mu\text{g}/\text{kg}$  to 4  $\mu\text{g}/\text{kg}$ . We divided the samples into ten groups based on their antibiotic concentrations. We generated bacterial association networks using sequencing data of 16S rRNA gene amplicons. We generated functional association networks using a large number of ARGs detected by a microarray-based tool named GeoChip (Shi et al., 2019). We aim to test three hypotheses: (i) Since high antibiotic stress reduces bacterial coexistence, bacterial networks would become more intricate with decreasing antibiotic concentrations; (ii) since high antibiotic stress enhances community resistance, functional networks would become less complex with decreasing antibiotic concentrations; and (iii) deterministic processes imposed by antibiotic stress would play less important roles in determining microbial interactions with decreasing antibiotic concentrations.

## 2. Materials and methods

### 2.1. Sample collection and measurements of geochemical factors

In April 2015, we collected four manure and four aerobic compost samples from each of five swine farms located in the suburban area of Beijing, China. We also collected four soil samples one month after compost amendment (compost-amended soil) from a nearby agricultural

field. Since compost could be further disseminated to neighboring soils, we collected four soil samples without compost amendment in the same agricultural field. Totally, 80 samples were collected (4 manure samples + 4 compost samples + 4 compost-amended soil samples + 4 unamended soil samples)  $\times$  5 swine farms. For each sample of compost-amended soil and unamended soil, three soil cores were taken at the 0–15 cm soil depth and thoroughly mixed to have enough samples for soil geochemistry and microbiology analyses. All samples were stored in a portable 4 °C refrigerator. After immediate transportation to the laboratory, each sample was divided into two parts: one was stored at 4 °C for analyses of antibiotic concentrations, and the other one was stored at –80 °C for microbial DNA extraction.

Soil temperature was in situ measured three times by thermometer and averaged for each sample. Similarly, water content was measured three times by hygrometer and averaged. We focused on several classes of antibiotics including tetracyclines (chlortetracycline, oxytetracycline, and tetracycline), sulfonamides (sulfadiazine, sulfadimidine, sulfamerazine, and sulfamethoxazole), and quinolones (norfloxacin and ofloxacin) because they are commonly used and employed in many large scale livestock practices (Yang and Carlson, 2003). Concentrations of those antibiotics were analyzed by a previously published method (Zhao et al., 2010). Briefly, 0.1 g of Na<sub>2</sub>EDTA and 10 ml of an extraction solution containing phosphate buffer (pH = 3.0) and acetonitrile (1:1 vol/vol) were used. After sonication for 30 min, samples were centrifuged at 7000  $\times$ g for 10 min. The soil extraction process was performed three times in each sample. The obtained supernatants were combined and then diluted to 500 ml with deionized water, filtered through 0.45  $\mu$ m filters, and acidified to pH 3.0 before solid-phase extraction. The samples were extracted using 6 ml of Oasis HLB extraction cartridges. Final extracts were transferred to 2 ml amber vials for analysis of liquid chromatography-MS/MS (ABI 3200 Q TRAP, Applied Biosystems, California, USA).

## 2.2. DNA extraction

DNA was extracted from 1.5 g of the sample by freeze-grinding and SDS-based lysis as described previously (Ding et al., 2015), and purified with a MoBio PowerSoil DNA isolation kit (MoBio Laboratories, Carlsbad, CA, USA) according to the manufacturer's protocol. DNA quality was assessed based on 260/280 nm and 260/230 nm absorbance ratios using a NanoDrop ND-1000 Spectrophotometer (NanoDrop Technologies Inc., Wilmington, DE, USA). Final DNA concentrations were quantified by PicoGreen using a FLUOstar Optima fluorescence plant reader (BMG Labtech, Jena, Germany). DNA was stored at –80 °C until further analyses.

## 2.3. Amplicon sequencing experiments and raw data analyses

The V4 hypervariable regions of 16S rRNA genes were amplified with the primer pair 515F (5'-GTGCCAGCMGCCGCGTAA-3') and 806R (5'-GGACTACHVGGGTWTCTAAT-3'). The sequencing experiment was carried out on a MiSeq platform (Illumina Inc., San Diego, CA, USA) using a 2  $\times$  150 pair-end format. Raw sequences were submitted to our Galaxy sequence analysis pipeline (<http://zhoulab5.rccc.ou.edu:8080>) (Wu et al., 2016). Raw sequences were assembled using FLASH. Joint sequences with an ambiguous base or a length of <245 bp were discarded for the 16S rRNA gene. After that, sequences were clustered into OTUs using UPARSE17 at 97% identity. Singletons and chimeras were removed from the remaining sequences. All sequences were randomly resampled to the depth of 31,109 sequences per sample.

## 2.4. GeoChip hybridization and raw data processing

The functional genes were analyzed with a microarray-based tool named GeoChip 5.0 (Agilent Technologies Inc., Santa Clara, CA, USA), which contains 9277 probes belonging to antibiotic resistance gene

families. Scanning of GeoChip hybridization and data processing were performed as described previously (Liu et al., 2015; Yue et al., 2015). In short, DNA samples were labeled with fluorescent dye Cy-3 dUTP and hybridized with GeoChip 5.0 in a rotator/incubator at 67 °C plus 10% formamide and rotated at 20 rpm for 24 h. After hybridization, the slides were scanned with a NimbleGen MS200 Microarray Scanner (Roche Inc., South San Francisco, CA, USA), and the scanned images were digitally extracted using the Agilent Feature Extraction software v11.5. Raw data were submitted to the Microarray Data Manager on the website (<http://ieg.ou.edu/microarray>) (Zhou et al., 2010). We removed spots with the signal-to-noise ratio below 2, which was considered to be of poor quality. Both the universal standard and functional gene spot intensities were used to normalize the signals among microarrays.

## 2.5. Network analyses

We divided 80 samples into ten groups according to the total concentration of nine categories of antibiotics, with each group containing eight samples (Table S1). The total antibiotic concentration decreased from Group 1 to Group 10. The common and rare OTUs/ARGs across samples in abundance versus prevalence plots are shown in Fig. S1. To minimize the possibility of false-positive results, only OTUs or ARGs detected in more than six samples of each group were used for the network construction following previous protocols (Wu et al., 2016). In brief, rank-based Spearman correlation, widely used for microbial network construction (Barberan et al., 2012; Weiss et al., 2016; Wu et al., 2016), was adopted to calculate the correlation matrix of OTUs or ARGs. The correlation matrix was then converted to a similarity matrix, which measures the degree of concordance between OTUs or ARGs across different samples by taking the absolute values of the correlation matrix (Yang et al., 2009). Then, random matrix theory (RMT) was used to automatically define the appropriate similarity threshold ( $St$ ) (Wu et al., 2016; Yang et al., 2009), which defines the minimal strength of the connections between each pair of nodes. RMT distinguishes system-specific, nonrandom associations from random associations and thus enables robustness of the network to random noise. In order to compare network topologies under the same condition, we used uniform  $St$  values to generate bacterial networks ( $St = 0.95$ ) and functional works ( $St = 0.98$ ). The uniform thresholds were determined by two criteria: (i) eigenvalues of the correlation matrices under this threshold followed the Poisson distribution; and (ii) the threshold was as low as possible (Yang et al., 2009). Subsequently, an adjacency matrix was obtained by retaining all the OTUs or ARGs whose similarity values were greater than the determined threshold.

A total of 100 random networks corresponding to each network were generated using the Molecular Ecological Network Analyses (MENA) pipeline (<http://ieg4.rccc.ou.edu/mena>). The numbers of nodes and links in random networks were constant, but all the links' positions were rewired randomly so that the rewired network was comparable to the empirical one (Maslov and Specificity, 2002). All network properties were calculated individually for each random network. The significance of network properties between the empirical and random networks was examined by Z-test using the 'BSDA' package in R. The topological properties of each network were characterized using the MENA pipeline. The topological properties included the total number of nodes, the total number of links, average degree (avgK), centralization of degree (CD), average clustering coefficient (avgCC), harmonic geodesic distance (HD), centralization of betweenness (CB), centralization of stress centrality (CS), network density, modularity, the number of positive and negative links, and proportion of positive and negative links. Detailed definitions of these properties are described in Table S2. All networks were graphed using Gephi v. 0.92 (Bastian et al., 2009). Nodes in the networks were classified into four categories according to within-module connectivity ( $Z_i$ ) and among-module connectivity ( $P_i$ ): network hubs (highly connected nodes within the entire network,

$Z_i > 2.5$  and  $P_i > 0.62$ ), module hubs (highly connected nodes within the modules,  $Z_i > 2.5$  and  $P_i \leq 0.62$ ), connectors (nodes that connect the modules,  $P_i > 0.62$ ), and peripherals (nodes connected in the modules with few links,  $Z_i < 2.5$  and  $P_i \leq 0.62$ ) (Olesen et al., 2007; Wu et al., 2016). Because network hubs, module hubs, and connectors have high within-module and among-module connectivity, they are regarded as putative keystone taxa.

To reduce the potential noise in network construction caused by the sample number, we also divided 80 samples into three groups (Group 1, Group 2, and Group 3) with decreasing antibiotic concentrations, with each group containing 27 or 26 samples. We then constructed both bacterial and functional networks for each group. The topological properties of those networks were calculated.

## 2.6. Statistical analyses

We calculated  $\alpha$ -diversity of bacterial and functional communities in each group with three indices (i.e., richness, Simpson index, and Inverse Simpson index), using the 'Picante' package in R. Pearson correlation was calculated to relate  $\alpha$ -diversity indices in each of 10 groups to average antibiotic concentrations, which were natural logarithmic transformed to normalize the data. 'Cor.test' function in the 'stats' package of R was used to calculate Pearson correlations.  $P$  values of Pearson correlations were adjusted by the 5% false discovery rate using 'p.adjust' function in the 'stats' R package.

We conducted the linear mixed-effects model with antibiotic concentration, soil water content, soil temperature, and sample type as fixed effects while sampling site as the random effect by using the 'lme4' R package. Wald type II  $\chi^2$  tests were used to calculate the  $P$  values from the linear models by using the 'car' R package. One-way ANOVA was conducted to test whether network properties differed between groups by using the 'aov' function in R. For each network property, the ANOVA model structure was set as a network property~order. The order was labeled as "high" for Group 1 to Group 5 and "low" for Group 6 to Group 10 in the ANOVA model according to average antibiotic concentrations of those groups.  $P$  values of the ANOVA models were adjusted using 'p.adjust' function in R. To determine which category of antibiotics best explained the observed variations in network properties, the random forest analysis was performed with 1000 permutations using 'randomforest' and 'rfPermute' packages (Banerjee et al., 2019). Antibiotics were regarded as predictors. The best predictors were identified based on their importance using 'importance' and 'varImpPlot' functions. An increase in node purity and mean square error were used to determine the significance of the predictors using the package 'randomForestExplainer' (Paluszynska and Biecek, 2017). Significant ( $P < 0.05$ ) predictors were presented.  $MSE_{OOB}$  was used to represent the mean squared out-of-bag error of the random forest model (Liaw and Wiener, 2001).

## 2.7. Ecological process analyses

To investigate the relative importance of deterministic and stochastic processes, we performed the null model analysis using abundance-weighted similarity metrics of bacterial OTUs, as shown previously (Stegen et al., 2013). First, we quantified the nearest-taxon index (NTI) using function 'ses.mntd' in the 'picante' package. NTI is the negative of the output of function 'ses.mntd', which quantifies the number of standard deviations that the observed mean nearest taxon distance is from the mean of the null distribution. NTI that is significantly different from zero indicates phylogenetic clustering (NTI > 0) or overdispersion (NTI < 0). Second, we quantified  $\beta$ NTI ( $\beta$  nearest-taxon index) for all pairwise community comparisons using an in-house pipeline (<http://166.111.42.42:8080/>) (Wu et al., 2016). The  $\beta$ NTI is based on a null model test of the phylogenetic  $\beta$  mean nearest-taxon distance characterizing the turnover in phylogenetic community composition. A value of  $|\beta$ NTI| > 2 indicates that the observed community assembly is

governed primarily by deterministic processes, while a value of  $|\beta$ NTI| < 2 indicates that the observed community assembly is governed primarily by stochastic processes.

## 3. Results

### 3.1. Bacterial taxa and ARGs

Alarming, all nine antibiotics measured here were detected in most of the samples (Table S1). Total concentrations of nine antibiotics decreased from 33,002  $\mu$ g/kg to 1  $\mu$ g/kg across samples. Based on the total concentration of antibiotics, we divided 80 samples into ten groups based on antibiotic concentrations, with eight samples in each group (Fig. S2). Soil water content and temperature were significantly ( $P < 0.05$  by Wilcox test) higher in manure and compost than in compost-amended soil and control soil (Fig. S3).

A total of 31,109 16S rRNA gene amplicon sequences were obtained, reaching saturation that was evident by the rarefaction curve (Fig. S4). Subsequently, 74,676 bacterial OTUs were generated based on the 97% identity criterion, with an average of 5447 OTUs per sample.  $\alpha$ -diversity indices (i.e., OTU richness, Shannon index, and inverse Simpson index) were negatively correlated ( $r = -0.81$  to  $-0.66$ ,  $P < 0.01$  by Pearson correlation) with antibiotic concentrations (Fig. S5), verifying that antibiotics imposed an adverse impact on bacterial communities. Bacterial community was correlated with nine antibiotics ( $r = 0.09$ – $0.35$ ,  $P < 0.05$  by Mantel test; Table S3) and soil water content ( $r = 0.23$ ,  $P < 0.05$ ), but not with soil temperature. There was a sharp transition of bacterial community composition from Group 5 to Group 6 (Fig. S6), wherein antibiotic concentrations were intermediate. Specifically, Group 1 to Group 5 was dominated by phylum *Firmicutes* (80%), followed by *Bacteroidetes* (8%) and *Proteobacteria* (5%). The largest three modules of bacterial networks were dominated by *Clostridiales* (69%), followed by orders *Bacteroidales* (9%) and *Lactobacillales* (8%) (Table S4). The most abundant phylum from Group 6 to Group 10 was *Proteobacteria* (37%), followed by *Actinobacteria* (18%) and *Acidobacteria* (15%) (Fig. S6). The most abundant orders (8%) in the largest three modules of bacterial networks were *Rhizobiales* and *Gp6*, followed by orders *Actinomycetales* (6%) and *Myxococcales* (6%) (Table S4).

A total of 9278 unique ARGs were detected, with an average of 5172 ARGs per sample. Relative abundances of 14 ARG categories were similar across ten groups (Fig. S7a), suggesting that functional potentials of antibiotic resistance were stable. Nonetheless,  $\alpha$ -diversity indices of ARGs (i.e., richness, Shannon index, and inverse Simpson index) were negatively correlated ( $r = -0.63$  to  $-0.52$ ,  $P < 0.05$  by Pearson correlation) with antibiotic concentrations (Fig. S7b), probably reflecting a reduced functional redundancy of ARGs at high antibiotic concentrations. ARGs were correlated with nine antibiotics ( $r = 0.12$ – $0.52$ ,  $P < 0.05$  by Mantel test; Table S3), but not with soil water content and soil temperature. The largest three modules of 10 functional networks were dominated by *MFS* efflux transporter genes (>56%), followed by *Mex* (>22%) and *ABC* (>4%) genes (Table S4).

### 3.2. Topological properties of association networks

We constructed bacterial networks and functional networks for each of the ten groups (Fig. 1). The network topology of bacterial and functional networks fit the power-law distribution very well (Tables S5 & S6), suggesting that only a few nodes of the networks outnumbered in links compared to the rest nodes of the networks (Wu et al., 2016). The bacterial and functional networks significantly ( $P < 0.05$  by Z-test) differed from corresponding random networks generated with the same numbers of nodes and links (Tables S5 & S6), suggesting that the observed network properties were nonrandom. The harmonic geodesic distance (HD) values of all networks were close to the logarithm of the number of network nodes, suggesting that those networks

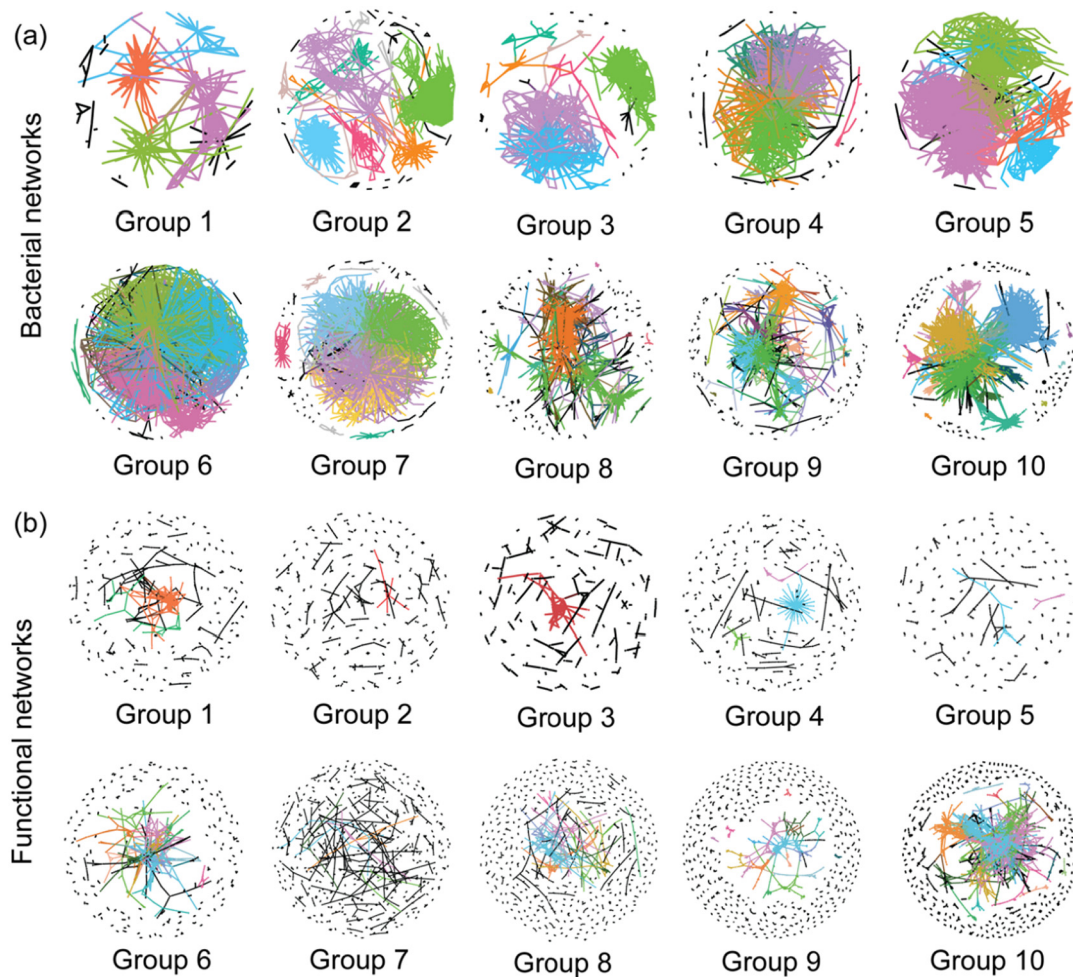


**Fig. 1.** (a) Bacterial and (b) functional networks divided into ten groups. Networks were constructed based on random matrix theory (RMT) algorithms. There are eight biological replicates in each group, wherein nodes represent OTUs in bacterial networks or ARGs in functional networks. Links between the nodes indicate significant correlations. Modules in each network are randomly colored, except that modules with less than ten nodes are colored in black.

possessed the typical property of a small world (Yang et al., 2017). Positive links accounted for more than 74% of all links in bacterial networks, except for the network of Group 6 containing only 47% positive links (Table S5). Therefore, most of the bacterial taxa tended to be co-occurring (i.e., positive links) rather than co-excluding (i.e., negative links). Similarly, positive links accounted for more than 56% of all links in functional networks (Table S6). Interestingly, functional networks of high antibiotic concentrations (from Group 1 to Group 5) only contained several links, resulting in isolated networks (Fig. 1).

The topological properties of bacterial and functional networks became substantially different among groups, as indicated by the ANOVA test (Table S7). The linear mixed-effect model showed that antibiotic concentrations exerted significant effects on topological properties of both bacterial ( $P = 0.04$  by Wald type II  $\chi^2$  test) and functional ( $P = 0.02$  by Wald type II  $\chi^2$  test) networks (Table 1). In contrast, the effects of other environmental factors, including sample type, soil water content, soil temperature, and the interactions among them, were not significant. The total number of nodes was negatively correlated ( $r = -0.91$ ,  $P < 0.05$  by Pearson correlation) with antibiotic concentrations in both bacterial and functional networks (Fig. 2), consistent with an expectation that high antibiotic stress decreased network sizes. As the number of nodes relates to the total link number, we showed that the average number of links per node was insignificantly correlated

**Table 1**

The main and interactive effects of environmental factors on bacterial and functional network properties by linear mixed-effects models.

	Df <sup>a</sup>	Bacterial network	Functional network
		<i>P</i>	<i>P</i>
LnTotal <sup>b</sup>	2	<b>0.04<sup>c</sup></b>	<b>0.02</b>
Water	2	0.99	0.99
Temp	1	0.79	0.78
Type	4	0.98	0.87
LnTotal × Water	1	0.89	0.72
LnTotal × Temp	1	0.70	0.81
Water × Temp	1	0.98	0.55
LnTotal × Type	3	0.85	0.76
Water × Type	3	0.99	0.98
Temp × Type	3	0.95	0.99
LnTotal × Water × Temp	1	0.82	0.90
LnTotal × Water × Type	3	0.98	0.99
LnTotal × Temp × Type	3	0.99	0.99
Water × Temp × Type	3	0.99	0.99
LnTotal × Water × Temp × Type	3	0.95	0.95

<sup>a</sup> Df: the degree of freedom.

<sup>b</sup> Abbreviations: LnTotal, the natural log-transformed total concentration of antibiotics; Water, soil water content (%); Temp, soil temperature; Type, sample types including manure, compost, compost-amended soil, and unamended agricultural soil.

<sup>c</sup> Significant ( $P < 0.05$ ) values are labeled in bold.

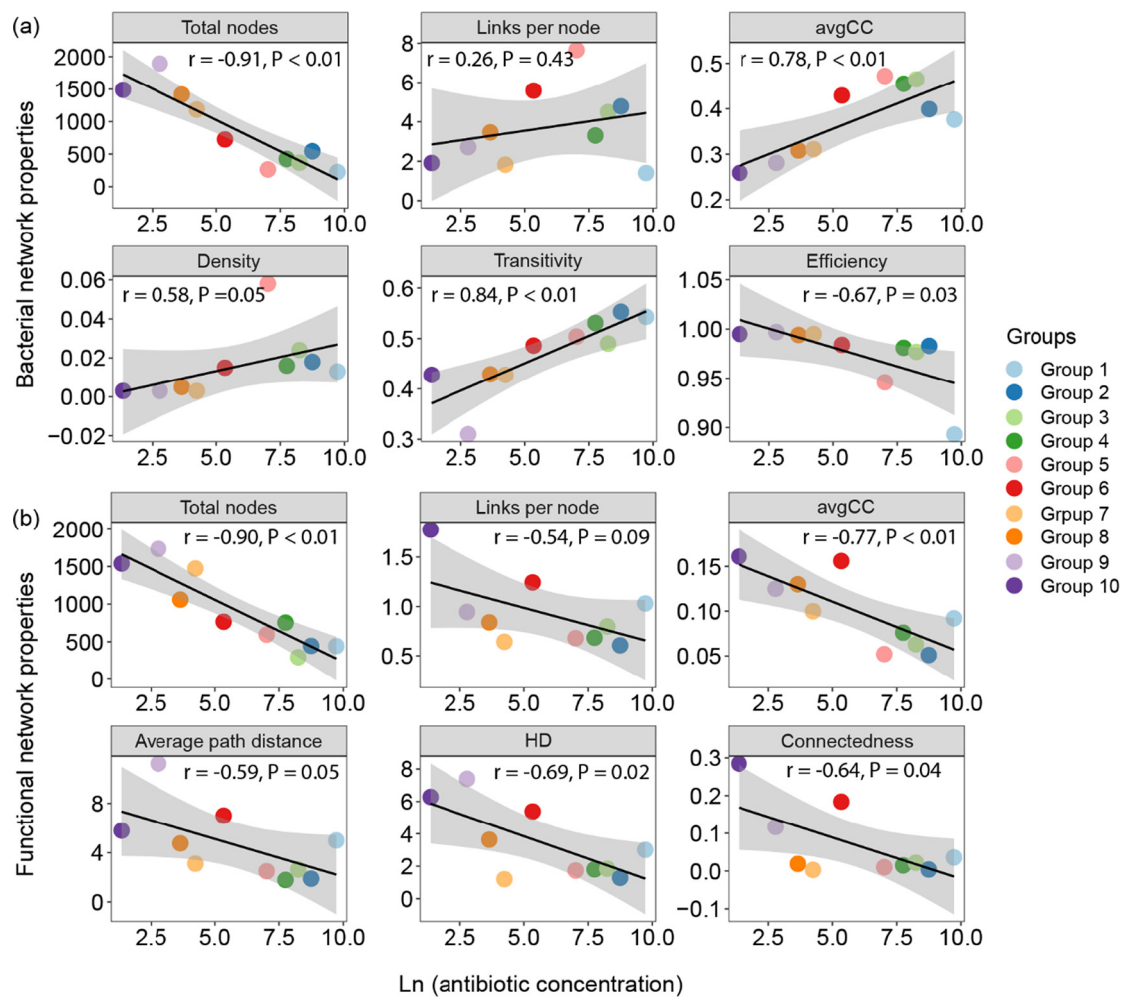


**Fig. 2.** Pearson correlations between antibiotic concentrations and selected topological properties of (a) bacterial and (b) functional networks. The topological properties of different networks are colored differently based on the group. Y-axis: values of network topological properties based on formulas in Table S2. AvgCC represents the average clustering coefficient, and HD represents harmonic geodesic distance.

( $P > 0.05$  by Pearson correlation) with antibiotic concentrations (Fig. 2). Nonetheless, the average clustering coefficient, density, and transitivity of bacterial networks were positively correlated ( $r = 0.58$ – $0.84$ ,  $P < 0.05$  by Pearson correlation) with antibiotic concentrations (Fig. 2a), suggesting that bacterial networks became less connected when antibiotic stress was lower. In contrast, topological properties of functional networks, including average clustering coefficient, average path distance, harmonic geodesic distance, and node connectedness, were negatively correlated ( $r = -0.77$  to  $-0.59$ ,  $P < 0.05$  by Pearson correlation) with antibiotic concentrations (Fig. 2b), suggesting that functional networks were more connected at lower antibiotic concentrations.

The networks of each group were reconstructed from only eight samples, which could have high noise because the number of  $n$  is small. To evaluate it, we re-divided all samples into three groups based on antibiotic concentrations. We showed that the total number of nodes of networks increased with lower antibiotic concentrations (Fig. S8). The average clustering coefficient and transitivity of bacterial networks decreased, while the average clustering coefficient, average path distance, and connectedness of functional networks increased with lower antibiotic concentrations (Fig. S8). The results suggested that the relationships between network properties and antibiotic concentrations were not affected by the number of samples used for network construction.

Random forest modeling revealed that ofloxacin best explained ( $P < 0.05$ ) average clustering coefficient, network density, and negative

link number of bacterial networks (Fig. S9a). In contrast, tetracycline best explained the average clustering coefficient, average path distance, and network connectedness of functional networks (Fig. S9b).

Modularity is a topological property to describe how well a community could be divided into modules (Wu et al., 2016). Both bacterial and functional networks were modular because the modularity values were significantly ( $P < 0.05$  by Z-test) higher than those of the corresponding randomized networks (Tables S5 & S6). The modularity values of bacterial networks ranged from 0.42 to 0.76, while that of functional networks ranged from 0.72 to 0.99 (Fig. 3). Interestingly, the modularity values of bacterial networks were humped (unimodal) in response to antibiotic concentrations (Fig. 3a), which was not observed in functional networks (Fig. 3b).

### 3.3. Putative keystone taxa and ARGs of association networks

Module hubs and connectors in bacterial networks from Group 1 to Group 5 were dominated by *Clostridiales* (67%), followed by *Lactobacillales* (13%) and *Bacteroidales* (9%) (Table S8). In networks from Group 6 to Group 10, 12% of module hubs and connectors belonged to *Clostridiales*, followed by *Gp6* (10%) and *Rhizobiales* (7%). Notably, only a few module hubs and connectors were present in more than one network (Table S9). OTU 1631 affiliated to the genus *Clostridium sensu stricto* was identified as a module hub in networks of Group 5 and Group 6. OTU 74513 affiliated to the genus *Sporobacter* was identified as a module hub in networks of Group 2 and Group 4.

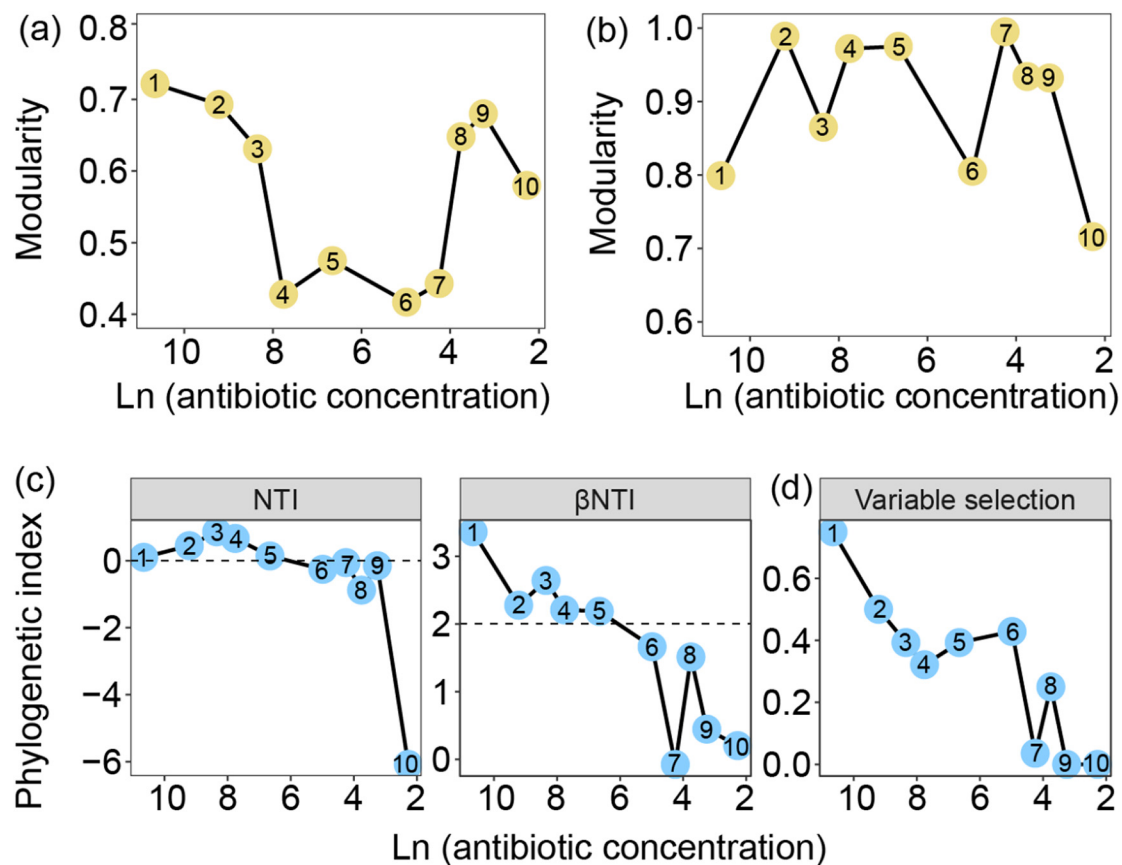


**Fig. 3.** (a) Variation in the modularity values of bacterial networks over ten groups; (b) variation in the modularity values of functional networks over ten groups; (c) variation in microbial phylogenetic indices of nearest taxon index (NTI),  $\beta$  nearest-taxon index ( $\beta$ NTI) over ten groups; and (d) variation in the explanation power of variable selection for bacterial community assembly over ten groups. Antibiotic concentrations are natural log-transformed. Group numbers are labeled in circles.

OTU 52794 affiliated to the genus *Rudaea* was identified as a module hub in networks of Group 7 and Group 10.

Only four network hubs were detected in bacterial networks. Among them, three network hubs, i.e., OTU 32445 affiliated to the genus *Terrisporobacter*, OTU 7034 affiliated to the genus *Clostridium sensu stricto* and OTU 140488 affiliated to the genus *Arthrobacter*, were present in the network of Group 6. OTU 98648 affiliated to the genus *Phascolarctobacterium* was a network hub of Group 4 (Table S9).

In functional networks,  $\beta$ -lactamase genes associated with  $\beta$ -lactamase resistance, ABC genes associated with ABC transporter ATP-binding, SMR genes associated with multidrug efflux system proteins, MATE genes associated with multidrug and toxic compound extrusion, tet genes associated with tetracycline resistance, Mex genes encoding multidrug resistance proteins, and MFS genes encoding drug resistance transporters were identified as module hubs or connectors (Fig. S7c). Unlike observations in bacterial networks, none of those keystone ARGs was present in more than one functional network. No network hub was detected in functional networks.

### 3.4. Ecological processes of bacterial community assemblies

To elucidate the underlying mechanism of the sharp transition of bacterial community composition from Group 5 to Group 6, we examined the relative importance of deterministic versus stochastic processes in shaping bacterial community assemblies. NTI values were significantly ( $P < 0.05$  by null model) higher than zero (Fig. 3c) from Group 1 to Group 5, showing the phylogenetic clustering of bacterial communities. The observed bacterial community turnover was significantly ( $P < 0.05$  by null model) greater than the null model expectation ( $|\beta$ NTI)  $> 2$ ), suggesting that deterministic processes were dominant for

the community assembly. In contrast, NTI values in Group 6 to Group 10 were significantly ( $P < 0.05$  by null model) lower than zero, showing phylogenetic over-dispersion of bacterial communities. The observed community turnover was significantly ( $P < 0.05$  by null model) less than the null model expectation ( $|\beta$ NTI)  $< 2$ ), suggesting that stochastic processes were dominant for the community assembly. A closer examination showed that the relative importance of variable selection decreased from 75% to 0.2% from Group 1 to Group 10 (Fig. 3d), which demonstrated that antibiotic selection was a major driver of bacterial communities at high antibiotic concentrations.

## 4. Discussion

With much of current work focusing on the diversity and composition of bacterial or functional communities, our understanding of microbial association networks, which represent potential ecological relationships within microbial communities, remains rudimentary. In the present study, bacterial networks were constructed with bacterial OTUs from 16S rRNA gene sequencing and functional networks were constructed with ARGs detected by GeoChip. The RMT-based networks are advantageous in its excellent capacity in tolerating noise (Luo et al., 2007), which is important for dealing with the large-scale data such as high-throughput sequencing and GeoChip. These networks can simplify complicated relationships among microbial members and identify keystone taxa with important roles in maintaining community structure and function (Power and Tilman, 1996; Wu et al., 2020). Thus, the networks provide a holistic angle for characterizing communities, considering the lack of other tractable methodologies in exploring species associations in diverse and largely uncultivated microbial communities (Zhou et al., 2011). However, the correlation-based association

networks may not represent physical interaction or cell-to-cell communication among microorganisms. Therefore, species associations and experimentally determined species interactions are often inconsistent (Barner et al., 2018).

The association networks delineate variations among nodes, which reflect their responses to environmental perturbations or shared niches (Shi et al., 2016). Network density, connectivity, and transitivity quantify how quickly the community responds to external perturbations because densely connected nodes coordinate better, rendering the network more resilient to perturbations (De Anda et al., 2018). Generally, higher antibiotic stress could lead to reduced diversity of microbial communities, which will simplify the community structure and reduce species connectivity (Kraemer et al., 2019). It could also hold true when concentrations of heavy metal or other organic pollutants are high (Kong et al., 2006; Szekeres et al., 2018), as they can be toxic for microorganisms. In the present study, we observed positive correlations between antibiotic concentrations and topological properties of average clustering coefficient, network density, and network transitivity of bacterial communities (Fig. 2a), suggesting that bacterial networks were more intensively connected and more robust to stress when antibiotic concentrations were high, which might be due to the following reasons.

Multidrug-resistant organisms can form interactive networks under antibiotic exposure, which aggravates risks of development and colonization of other resistant microorganisms (Wang et al., 2017). When exposed to antibiotics, a small number of resistant cells of *Escherichia coli* can protect other vulnerable cells by producing indole, which acted as a cell-signaling chemical (Lee et al., 2010). As a result, antibiotics could foster greater direct and indirect interactions among bacteria. Nonetheless, it is also likely that some of the synchronized variations in bacterial networks represent niche sharing between taxa (Berry and Widder, 2014). Therefore, more bacterial network connectivity at high antibiotic concentrations (Fig. 2a) could result from both intensive taxa interactions and the development of shared guilds or niches. In contrast, connectivity among ARGs (i.e., average clustering coefficient) was negatively correlated with antibiotic concentrations (Fig. 2b), probably reflecting a reduced functional redundancy owing to antibiotic selection. The decreased connectivity among ARGs might be attributed to the decreased number of ARGs caused by taxa loss. Antagonistic interactions among different antibiotics can also reduce the functional redundancy of ARGs (Yeh et al., 2009).

Topological properties of bacterial networks were best explained by ofloxacin (Fig. S9a), one of the most commonly used fluoroquinolone antibiotics for animal disease control (Massé et al., 2014). Ofloxacin degrades very slowly and could persist in the environment for a long time (Massé et al., 2014). However, fluoroquinolone-resistant bacteria could survive high concentrations of ofloxacin and repopulated after ofloxacin treatment ceased (Gardner et al., 2004). Therefore, our finding of the significant impact of ofloxacin on bacterial interactions could serve as a hitherto overlooked mechanism to facilitate the transfer of ARGs. In contrast, the topological properties of functional networks were best explained by tetracycline (Fig. S9b). We detected highly abundant *MFS* efflux genes in functional networks (Fig. S7a), which was vital for soil bacteria resistance to tetracycline via detoxification of metabolic intermediates, virulence, and signal trafficking (Gibson et al., 2014; Sailer et al., 2003).

Keystone taxa are highly connected taxa, which affect the network stability substantially when they are removed. The majority of keystone bacterial taxa belong to the order *Clostridiales*, many of which are well known as opportunistic pathogens that produce toxic chemicals (Africa et al., 2014). OTU 1631 from the genus *Clostridium* sensu stricto was a module hub in bacterial networks of Group 5 and Group 6 (Table S9), unveiling potential risks of pathophoresis through taxa connections. OTU 74513 from the genus *Sporobacter* was also identified as a module hub in bacterial networks of Group 2 and Group 4. *Sporobacter* can grow exclusively on a limited range of aromatic compounds, which facilitate its survival at high antibiotic concentrations (Grechmora et al., 1996).

Mathematically, network modularity can predict system failure since higher modularity enhances system resilience of both natural and constructed networks by reducing signal cascades (Haldane and May, 2011). More specifically, high modularity could provide an advantage for bacterial communities to be more resilient to antibiotic stress (Newman, 2006). As bacterial network modularity decreased dramatically at the intermediate antibiotic concentration (Fig. 3a), it could be a sensitive indicator for bacterial community variations in response to environmental perturbation. Both heterogeneity and connectivity of nodes are strongly related to network modularity (van Nes and Scheffer, 2005). In a community wherein taxonomic diversity is high, a modular feature allows different groups of taxa to perform independent functions, resulting in less overlap and connectivity among bacterial taxa (Faust and Raes, 2012). As a result, the network can be robust and resilient to environmental perturbation. As connectivity (i.e., average clustering coefficient in Fig. 2a) of bacterial networks further increased with increasing antibiotic concentrations, highly connected networks could easily cascade into a systemic transition when a local perturbation occurs (van Nes and Scheffer, 2005).

Ecological processes are key mechanisms for altering microbial community compositions, thus interactions among microbes (Wong et al., 2017). High antibiotic concentrations select for phylogenetically conserved bacterial taxa (Fig. 3c), which could form clusters of densely interacting nodes that perform similar functions or share similar niches (Sharan and Ideker, 2006). The resulting networks have high inner connectivity within modules while being loosely connected to the rest of the network, leading to high modularity of the network (Bebek and Yang, 2007; Erten et al., 2009; Koyutürk et al., 2006). In contrast, taxa may randomly interact within and among themselves, which helps maintain network stability when most connected nodes are removed from the network (Memmott et al., 2004). Therefore, the shift from deterministic processes to stochastic processes might confer robustness to the bacterial community compositions undergoing considerable changes from Group 5 to Group 6 (Fig. S6).

To validate those observations experimentally, one can explore a bottom-up approach designing community with known species that grow on culture mediums with decreasing gradient of antibiotic concentrations. The association networks based on the experimental data can be compared with the empirical networks. Community assembly mechanisms could also be inferred from the experimental data and compared with the empirical assemblies.

The nature of the amplicon-based data, such as compositionality and sparsity, could bring in spurious correlations in the network (Gloor et al., 2017; Layeghifard et al., 2017). The compositional effects should be considered for communities with low effective numbers of species (inverse Simpson index < 13), but it is suggested that the effects are generally insignificant for highly diverse communities (Weiss et al., 2016), which is verified here since the inverse Simpson index of bacterial communities is larger than 17 across samples and that of ARGs is larger than 300 (Figs. S5 & S7). We also accounted for some of the sparsity by filtering out rare OTUs prior to network construction. Additionally, the different sample types did not evenly represent different microbial groups in our study, owing to different nutrient levels and physical properties of samples. It was recently shown that antibiotic pollution-induced community tolerance was enhanced upon additional soil amendment with fresh pig slurry, signifying the importance of sample types in affecting microbial communities (Schmitt et al., 2005).

## 5. Conclusions

Our study highlights that bacterial networks became more connected in environments with higher antibiotic concentrations, which may facilitate the transmission of antibiotic resistance within microbial communities. Bacterial communities have undergone huge taxonomic composition changes along the antibiotic transmission chain, and the network modularity was a good indicator of the community changes

in response to antibiotics. Shifts in microbial community assembly processes were identified as the possible mechanisms underlying the dynamics of microbial interactions. Collectively, our study signifies the potential roles of microbial interactions in tracking the transmission of antibiotic resistance in the environment.

### CRedit authorship contribution statement

**Qun Gao:** Conceptualization, Methodology, Investigation, Visualization, Writing - original draft. **Shuhong Gao:** Writing - review & editing. **Colin Bates:** Writing - review & editing. **Yufei Zeng:** Investigation. **Jiesi Lei:** Investigation. **Hang Su:** Investigation. **Qiang Dong:** Investigation. **Ziyan Qin:** Investigation. **Jianshu Zhao:** Investigation. **Qijuting Zhang:** Investigation. **Daliang Ning:** Methodology, Software. **Yi Huang:** Resources. **Jizhong Zhou:** Writing - review & editing. **Yunfeng Yang:** Writing - review & editing, Supervision, Conceptualization, Funding acquisition.

### Declaration of competing interest

The authors declare that they have no known competing financial interests or personal relationships that could have appeared to influence the work reported in this paper.

### Acknowledgments

This work was supported by the China National Key R&D Program [grant number 2019YFC1806204], the National Natural Science Foundation of China [grant numbers 41877048, 41825016], and the State Key Joint Laboratory of Environment Simulation and Pollution Control [grant number 19L01ESPC].

### Data availability

DNA sequences of 16S rRNA genes are available in the NCBI Sequence Read Archive under project no. PRJNA516026. ARG Data are available in the NCBI GEO database under project no. GSE132839.

### References

Africa, C., Nel, J., Stemmet, M., 2014. Anaerobes and bacterial vaginosis in pregnancy: virulence factors contributing to vaginal colonisation. *Int. J. Environ. Res. Public Health* 11, 6979–7000.

Allen, H.K., 2014. Antibiotic resistance gene discovery in food-producing animals. *Curr. Opin. Microbiol.* 19, 25–29.

Balcazar, J.L., 2014. Bacteriophages as vehicles for antibiotic resistance genes in the environment. *PLoS Pathog.* 10, e1004219.

Banerjee, S., Walder, F., Büchi, L., Meyer, M., Held, A.Y., Gatterger, A., et al., 2019. Agricultural intensification reduces microbial network complexity and the abundance of keystone taxa in roots. *The ISME journal* 13, 1722–1736.

Barberan, A., Bates, S.T., Casamayor, E.O., Fierer, N., 2012. Using network analysis to explore co-occurrence patterns in soil microbial communities. *ISME J* 6, 343–351.

Barner, A.K., Coblenz, K.E., Hacker, S.D., Menge, B.A., 2018. Fundamental contradictions among observational and experimental estimates of non-trophic species interactions. *Ecology* 99, 557–566.

Bastian, M., Heymann, S., Jacomy, M., 2009. Gephi: an open source software for exploring and manipulating networks. *Third International AAAI Conference on Weblogs and Social Media*, pp. 361–362.

Bebek, G., Yang, J., 2007. PathFinder: mining signal transduction pathway segments from protein-protein interaction networks. *BMC bioinformatics* 8, 335–348.

Bengtsson-Palme, J., 2017. Antibiotic resistance in the food supply chain: where can sequencing and metagenomics aid risk assessment? *Curr. Opin. Food Sci.* 14, 66–71.

Bengtsson-Palme, J., Larsson, D.G.J., 2015. Antibiotic resistance genes in the environment: prioritizing risks. *Nat. Rev. Microbiol.* 13, 396.

Bengtsson-Palme, J., Boulund, F., Fick, J., Kristiansson, E., Larsson, D.G.J., 2014. Shotgun metagenomics reveals a wide array of antibiotic resistance genes and mobile elements in a polluted lake in India. *Front. Microbiol.* 5, 648.

Bengtsson-Palme, J., Hammarén, R., Pal, C., Östman, M., Björleinius, B., Flach, C.-F., et al., 2016. Elucidating selection processes for antibiotic resistance in sewage treatment plants using metagenomics. *Sci. Total Environ.* 572, 697–712.

Bengtsson-Palme, J., Kristiansson, E., Larsson, D.G.J., 2017. Environmental factors influencing the development and spread of antibiotic resistance. *FEMS Microbiol. Rev.* 42,

Berry, D., Widder, S., 2014. Deciphering microbial interactions and detecting keystone species with co-occurrence networks. *Front. Microbiol.* 5, 219.

Cabello, F.C., 2006. Heavy use of prophylactic antibiotics in aquaculture: a growing problem for human and animal health and for the environment. *Environ. Microbiol.* 8, 1137–1144.

De Anda, V., Zapata-Peñasco, I., Blaz, J., Poot-Hernandez, A.C., Contreras-Moreira, B., González-Laffitte, M., et al., 2018. Understanding the mechanisms behind the response to environmental perturbation in microbial mats: a metagenomic-network based approach. *Front. Microbiol.* 9, 1–24.

Ding, J., Zhang, Y., Wang, M., Sun, X., Cong, J., Deng, Y., et al., 2015. Soil organic matter quantity and quality shape microbial community compositions of subtropical broadleaved forests. *Mol. Ecol.* 24, 5175–5185.

Erten, S., Li, X., Bebek, G., Li, J., Koyutürk, M., 2009. Phylogenetic analysis of modularity in protein interaction networks. *BMC bioinformatics* 10, 333–347.

Faust, K., Raes, J., 2012. Microbial interactions: from networks to models. *Nat. Rev. Microbiol.* 10, 538–550.

Gardner, T.S., Di Bernardo, D., Lorenz, D., Collins, J.J., 2003. Inferring genetic networks and identifying compound mode of action via expression profiling. *Science* 301, 102–105.

Gardner, T.S., Shimer, S., Collins, J.J., 2004. Inferring microbial genetic networks. *ASM News* 70, 121–126.

Gibson, M.K., Forsberg, K.J., Dantas, G., 2014. Improved annotation of antibiotic resistance determinants reveals microbial resistomes cluster by ecology. *The ISME Journal* 9, 207–216.

Gloor, G.B., Macklaim, J.M., Pawlowsky-Glahn, V., Egozcue, J.J., 2017. Microbiome datasets are compositional: and this is not optional. *Front. Microbiol.* 8.

Goh, E.-B., Yim, G., Tsui, W., McClure, J., Surette, M.G., Davies, J., 2002. Transcriptional modulation of bacterial gene expression by subinhibitory concentrations of antibiotics. *Proc. Natl. Acad. Sci.* 99, 17025–17030.

Grech-mora, I., Fardeau, M.-L., Patel, B.K.C., Ollivier, B., Rimbault, A., Prensier, G., et al., 1996. Isolation and characterization of *Sporobacter termitidis* gen. nov., sp. nov., from the digestive tract of the wood-feeding termite *Nasutitermes lujae*. *Int. J. Syst. Evol. Microbiol.* 46, 512–518.

Haldane, A.G., May, R.M., 2011. Systemic risk in banking ecosystems. *Nature* 469, 351–355.

Hui, C., Richardson, D.M., Pyšek, P., Le Roux, J.J., Kučera, T., Jarošík, V., 2013. Increasing functional modularity with residence time in the co-distribution of native and introduced vascular plants. *Nat. Commun.* 4, 2454–2462.

Kelsic, E.D., Zhao, J., Vetsigian, K., Kishony, R., 2015. Counteraction of antibiotic production and degradation stabilizes microbial communities. *Nature* 521, 516–519.

Kohanski, M.A., Dwyer, D.J., Hayete, B., Lawrence, C.A., Collins, J.J., 2007. A common mechanism of cellular death induced by bactericidal antibiotics. *Cell* 130, 797–810.

Kohanski, M.A., Dwyer, D.J., Wierzbowski, J., Cottarel, G., Collins, J.J., 2008. Mistranslation of membrane proteins and two-component system activation trigger antibiotic-mediated cell death. *Cell* 135, 679–690.

Kong, W.D., Zhu, Y.G., Fu, B.J., Marschner, P., He, J.Z., 2006. The veterinary antibiotic oxytetracycline and Cu influence functional diversity of the soil microbial community. *Environ. Pollut.* 143, 129–137.

Koyutürk, M., Kim, Y., Subramaniam, S., Szpankowski, W., Grama, A., 2006. Detecting conserved interaction patterns in biological networks. *J. Comput. Biol.* 13, 1299–1322.

Kraemer, S.A., Ramachandran, A., Perron, G.G., 2019. Antibiotic pollution in the environment: from microbial ecology to public policy. *Microorganisms* 7, 180.

Layeghifard, M., Hwang, D.M., Guttman, D.S., 2017. Disentangling interactions in the microbiome: a network perspective. *Trends Microbiol.* 25, 217–228.

Lee, H.H., Molla, M.N., Cantor, C.R., Collins, J.J., 2010. Bacterial charity work leads to population-wide resistance. *Nature* 467, 82–85.

Li, B., Yang, Y., Ma, L., Ju, F., Guo, F., Tiedje, J.M., et al., 2015. Metagenomic and network analysis reveal wide distribution and co-occurrence of environmental antibiotic resistance genes. *The ISME Journal* 9, 2490–2502.

Liaw, A., Wiener, M., 2001. Classification and regression by RandomForest. *R news* 2, 18–22.

Linares, J.F., Gustafsson, I., Baquero, F., Martinez, J., 2006. Antibiotics as intermicrobial signaling agents instead of weapons. *Proc. Natl. Acad. Sci.* 103, 19484–19489.

Liu, S., Wang, F., Xue, K., Sun, B., Zhang, Y., He, Z., et al., 2015. The interactive effects of soil transplant into colder regions and cropping on soil microbiology and biogeochemistry. *Environ. Microbiol.* 17, 566–576.

Lundström, S.V., Östman, M., Bengtsson-Palme, J., Rutgersson, C., Thoudal, M., Sircar, T., et al., 2016. Minimal selective concentrations of tetracycline in complex aquatic bacterial biofilms. *Sci. Total Environ.* 553, 587–595.

Luo, F., Yang, Y., Zhong, J., Gao, H., Khan, L., Thompson, D.K., et al., 2007. Constructing gene co-expression networks and predicting functions of unknown genes by random matrix theory. *BMC Bioinformatics* 8, 299.

Macheleidt, J., Mattern, D.J., Fischer, J., Netzker, T., Weber, J., Schroeckh, V., et al., 2016. Regulation and role of fungal secondary metabolites. *Annu. Rev. Genet. Evol. Syst.* 50, 371–392.

Maslov, S., Specificity, Snejden K., 2002. Stability in topology of protein networks. *Science* 296, 910–913.

Massé, D.I., Saady, N.M.C., Gilbert, Y., 2014. Potential of biological processes to eliminate antibiotics in livestock manure: an overview. *Animals* 4, 146–163.

Memmott, J., Waser, N.M., Price, M.V., 2004. Tolerance of pollination networks to species extinctions. *Proc. R. Soc. Lond. Ser. B Biol. Sci.* 271, 2605–2611.

Narisawa, N., Haruta, S., Arai, H., Ishii, M., Igarashi, Y., 2008. Coexistence of antibiotic-producing and antibiotic-sensitive bacteria in biofilms is mediated by resistant bacteria. *Appl. Environ. Microbiol.* 74, 3887–3894.

van Nes, E.H., Scheffer, M., 2005. Implications of spatial heterogeneity for catastrophic regime shifts in ecosystems. *Ecology* 86, 1797–1807.

Newman, M.E., 2006. Modularity and community structure in networks. *Proc. Natl. Acad. Sci.* 103, 8577–8582.

- Ning, D., Deng, Y., Tiedje, J.M., Zhou, J., 2019. A general framework for quantitatively assessing ecological stochasticity. *Proc. Natl. Acad. Sci.* 116, 16892–16898.
- Olesen, J.M., Bascompte, J., Dupont, Y.L., Jordano, P., 2007. The modularity of pollination networks. *Proc. Natl. Acad. Sci.* 104, 19891.
- Paluszynska, A., Biecek, P., 2017. randomForestExplainer: explaining and visualizing random forests in terms of variable importance. R package version 0.9.
- Poirel, L., Rodriguez-Martinez, J.-M., Mammeri, H., Liard, A., Nordmann, P., 2005. Origin of plasmid-mediated quinolone resistance determinant QnrA. *Antimicrob. Agents Chemother.* 49, 3523–3525.
- Power, Mary E., Tilman, David, 1996. Challenges in the quest for keystones. *BioScience* 46, 609–620.
- Rizzo, L., Manaia, C., Merlin, C., Schwartz, T., Dagot, C., Ploy, M.C., et al., 2013. Urban wastewater treatment plants as hotspots for antibiotic resistant bacteria and genes spread into the environment: a review. *Sci. Total Environ.* 447, 345–360.
- Rolain, J.-M., 2013. Food and human gut as reservoirs of transferable antibiotic resistance encoding genes. *Front. Microbiol.* 4, 173.
- Rumbaugh, K.P., Diggle, S.P., Watters, C.M., Ross-Gillespie, A., Griffin, A.S., West, S.A., 2009. Quorum sensing and the social evolution of bacterial virulence. *Curr. Biol.* 19, 341–345.
- Sailer, F.C., Meberg, B.M., Young, K.D., 2003.  $\beta$ -Lactam induction of colanic acid gene expression in *Escherichia coli*. *FEMS Microbiol. Lett.* 226, 245–249.
- Schmitt, H., Haapakangas, H., van Beelen, P., 2005. Effects of antibiotics on soil microorganisms: time and nutrients influence pollution-induced community tolerance. *Soil Biol. Biochem.* 37, 1882–1892.
- Sharan, R., Ideker, T., 2006. Modeling cellular machinery through biological network comparison. *Nat. Biotechnol.* 24, 427–433.
- Shi, S., Nuccio, E.E., Shi, Z.J., He, Z., Zhou, J., Firestone, M.K., 2016. The interconnected rhizosphere: high network complexity dominates rhizosphere assemblages. *Ecol. Lett.* 19, 926–936.
- Shi, Z., Yin, H., Van Nostrand, J.D., Voordeckers, J.W., Tu, Q., Deng, Y., et al., 2019. Functional gene array-based ultrasensitive and quantitative detection of microbial populations in complex communities. *mSystems* 4, e00296-19.
- Stegen, J.C., Lin, X., Fredrickson, J.K., Chen, X., Kennedy, D.W., Murray, C.J., et al., 2013. Quantifying community assembly processes and identifying features that impose them. *The ISME Journal* 7, 2069–2079.
- Szekeres, E., Chiriac, C.M., Baricz, A., Szóke-Nagy, T., Lung, I., Soran, M.-L., et al., 2018. Investigating antibiotics, antibiotic resistance genes, and microbial contaminants in groundwater in relation to the proximity of urban areas. *Environ. Pollut.* 236, 734–744.
- Wang, J., Foxman, B., Mody, L., Snitkin, E.S., 2017. Network of microbial and antibiotic interactions drive colonization and infection with multidrug-resistant organisms. *Proc. Natl. Acad. Sci.* 114, 10467–10472.
- Wang, F., Han, W., Chen, S., Dong, W., Qiao, M., Hu, C., et al., 2020. Fifteen-year application of manure and chemical fertilizers differently impacts soil ARGs and microbial community structure. *Front. Microbiol.* 11, 62.
- Weiss, S., Van Treuren, W., Lozupone, C., Faust, K., Friedman, J., Deng, Y., et al., 2016. Correlation detection strategies in microbial data sets vary widely in sensitivity and precision. *ISME J* 10, 1669–1681.
- Wong, H.L., Visscher, P.T., White Iii, R.A., Smith, D.-L., Patterson, M.M., Burns, B.P., 2017. Dynamics of archaea at fine spatial scales in Shark Bay mat microbiomes. *Sci. Rep.* 7, 46160.
- Wu, L., Yang, Y., Chen, S., Zhao, M., Zhu, Z., Yang, S., et al., 2016. Long-term successional dynamics of microbial association networks in anaerobic digestion processes. *Water Res.* 104, 1–10.
- Wu, L., Shan, X., Chen, S., Zhang, Q., Qi, Q., Qin, Z., et al., 2020. Progressive microbial community networks with incremental organic loading rates underlie higher anaerobic digestion performance. *mSystems* 5, e00357-19.
- Xavier, J.B., 2011. Social interaction in synthetic and natural microbial communities. *Mol. Syst. Biol.* 7, 483–493.
- Yang, S., Carlson, K., 2003. Evolution of antibiotic occurrence in a river through pristine, urban and agricultural landscapes. *Water Res.* 37, 4645–4656.
- Yang, Y., Harris, D.P., Luo, F., Xiong, W., Joachimiak, M., Wu, L., et al., 2009. Snapshot of iron response in *Shewanella oneidensis* by gene network reconstruction. *BMC Genomics* 10, 131.
- Yang, S., Zhang, Y., Cong, J., Wang, M., Zhao, M., Lu, H., et al., 2017. Variations of soil microbial community structures beneath broadleaved forest trees in temperate and subtropical climate zones. *Front. Microbiol.* 8, 200–209.
- Yeh, P.J., Hegreness, M.J., Aiden, A.P., Kishony, R., 2009. Drug interactions and the evolution of antibiotic resistance. *Nat. Rev. Microbiol.* 7, 460–466.
- Yue, H., Wang, M., Wang, S., Gilbert, J.A., Sun, X., Wu, L., et al., 2015. The microbe-mediated mechanisms affecting topsoil carbon stock in Tibetan grasslands. *The ISME Journal* 9, 2012–2020.
- Zhang, Y., Hao, X., Alexander, T.W., Thomas, B.W., Shi, X., Lupwayi, N.Z., 2018. Long-term and legacy effects of manure application on soil microbial community composition. *Biol. Fertil. Soils* 54, 269–283.
- Zhang, Y.-J., Hu, H.-W., Chen, Q.-L., Singh, B.K., Yan, H., Chen, D., et al., 2019a. Transfer of antibiotic resistance from manure-amended soils to vegetable microbiomes. *Environ. Int.* 130, 104912.
- Zhang, Z., Deng, Y., Feng, K., Cai, W., Li, S., Yin, H., et al., 2019b. Deterministic assembly and diversity gradient altered the biofilm community performances of bioreactors. *Environmental science & technology* 53, 1315–1324.
- Zhang, M., He, L.-Y., Liu, Y.-S., Zhao, J.-L., Zhang, J.-N., Chen, J., et al., 2020. Variation of antibiotic resistome during commercial livestock manure composting. *Environ. Int.* 136, 105458.
- Zhao, L., Dong, Y.H., Wang, H., 2010. Residues of veterinary antibiotics in manures from feedlot livestock in eight provinces of China. *Sci. Total Environ.* 408, 1069–1075.
- Zhao, J., Gao, Q., Zhou, J., Wang, M., Liang, Y., Sun, B., et al., 2019. The scale dependence of fungal community distribution in paddy soil driven by stochastic and deterministic processes. *Fungal Ecol.* 42, 100856.
- Zhou, J., Deng, Y., Luo, F., He, Z., Tu, Q., Zhi, X., 2010. Functional molecular ecological networks. *mBio* 1, e00169-10.
- Zhou, J., Deng, Y., Luo, F., He, Z., Yang, Y., 2011. Phylogenetic molecular ecological network of soil microbial communities in response to elevated CO<sub>2</sub>. *mBio* 2, e00122-11.
- Zhou, J., Deng, Y., Zhang, P., Xue, K., Liang, Y., Van Nostrand, J.D., et al., 2014. Stochasticity, succession, and environmental perturbations in a fluidic ecosystem. *Proc. Natl. Acad. Sci.* 111, E836–E845.